HHS Public Access

Author manuscript

Chem Commun (Camb). Author manuscript; available in PMC 2018 August 22.

Published in final edited form as:

Chem Commun (Camb). 2017 August 22; 53(68): 9394–9397. doi:10.1039/c7cc04291d.

Zinc-coordination and C-peptide complexation: a potential mechanism for the endogenous inhibition of IAPP aggregation

Xinwei Ge[a,†], **Aleksandr Kakinen**[b,†], **Esteban N. Gurzov**[c,d], **Wen Yang**[e], **Lokman Pang**[c,d], **Emily H. Pilkington**[b], **Praveen Govindan-Nedumpully**[a], **Pengyu Chen**[e], **Frances Separovic**[f], **Thomas P. Davis**[b,g], **Pu Chun Ke**[b], and **Feng Ding**[a]

[a]Department of Physics and Astronomy, Clemson University, Clemson, SC 29634, USA

[b]ARC Centre of Excellence in Convergent Bio-Nano Science and Technology, Monash Institute of Pharmaceutical Sciences, Monash University, 381 Royal Parade, Parkville, VIC 3052, Australia

[c]St Vincent's Institute of Medical Research, 9 Princes Street, Fitzroy, VIC 3065, Australia

[d]Department of Medicine, St. Vincent's Hospital, University of Melbourne, Melbourne, Australia

[e]Department of Material Engineering, Auburn, AL 36849, USA

[f]School of Chemistry, Bio21 Institute, University of Melbourne, Melbourne, Victoria 3010, Australia

[g]Department of Chemistry, Warwick University, Gibbet Hill, Coventry, CV4 7AL, United Kingdom

Abstract

Aggregation of the highly amyloidogenic IAPP is endogenously inhibited inside beta-cell granules at millimolar concentrations. Combining *in vitro* experiments and computer simulations, we demonstrated that the stabilization of IAPP upon the formation of zinc-coordinated ion molecular complex with C-peptide might be important for the endogenous inhibtion of IAPP aggregation.

Graphical abstract

Zinc-coordination and C-peptide complexation stabilize IAPP and inhibit its amyloid aggregation

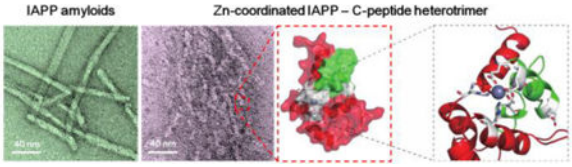

Correspondence to: Thomas P. Davis; Pu Chun Ke; Feng Ding.

†XG and AK cortributed equally to the work.

Electronic Supplementary Information (ESI) available: [details of any supplementary information available should be included here]. See DOI: 10.1039/x0xx00000x

Author contributions: FD, PK, and TPD conceived the project. AK performed the TEM experiment and conducted statistical analysis; AK and EHP performed the ThT assay and data analysis; WY and PC performed and analysed CD measurements. XG, PGN and FD performed DMD simulations and data analysis. EG and LP conducted the viability assay and analysis. XG, PK, FD and AK wrote the paper. All authors discussed the data and agreed on the manuscript.

The amyloid aggregation[1–3] of islet amyloid polypeptide (IAPP), a 37-residue peptide hormone co-synthesized, co-stored, and co-secreted with insulin by pancreatic β-cells for glycemic control,[4] is associated with β-cell death in type-2 diabetes (T2D).[5,6] IAPP readily forms amyloid fibrils *in vitro* within hours at μMconcentrations.[7] However, before its secretion to the bloodstream IAPP is stored inside β-cell granules at *m*M concentrations for hours without apparent aggregation in healthy individuals. Therefore, the unique physiological environment of β-cell granules - e.g., low pH[7,8] and high concentrations of zinc ions (Zn^{2+}), insulin and C-peptide[9] - *endogenously inhibits* IAPP aggregation. The high concentration of Zn^{2+}, maintained by β-cell-specific zinc transporters - ZnT8,[10] is important for the efficient storage of insulin in β-cells. Zn^{2+} coordinates the formation of insulin hexamers, which constitute insulin crystals as the dense core of β-cell granules.[11] C-peptide is a proteolytic product of proinsulin and has been recently found to play important physiological roles in addition to a marker of insulin production.[12] Inhibition of IAPP aggregation by insulin[13] and low pH[14,15] has been observed *in vitro*. Electrostatic repulsion between protonated histidine18 (His18) was found responsible for inhibiting IAPP aggregation at low pH.[14,16] Previous studies by our group and others[17–19] offered molecular insights to the binding of insulin with IAPP for understanding the inhibition mechanism. The inhibition of IAPP aggregation by insulin has also been found to suppress the aggregation-induced membrane disruption.[20] However, because the pH of β-cell granules (~5.5 pH) is close to the isoelectric point of His18[8,21] (i.e., a significantly high portion of IAPP is still unprotonated and aggregation-prone) and also because IAPP is found exclusively in the soluble halo fraction of β-cell granules while insulin is mostly insoluble in the core (i.e., inaccessible for IAPP aggregation inhibition),[22] a balance of Zn^{2+} and C-peptide co-localized with IAPP appears crucial for maintaining the native state of IAPP in addition to the low pH effect.[15]

NMR experiments have shown that Zn^{2+} binds the His18 of IAPP and coordinates the formation of IAPP oligomers.[23–25] Discrete molecular dynamics (DMD) simulations of zinc-coordinated IAPP oligomers with different molecular weights (MWs)[16] revealed that high MW IAPP oligomers (enriched at low zinc/IAPP stoichiometry) could form inter-peptide hydrogen bonds and enhance the formation of β-rich aggregates, but electrostatic repulsions between zinc-bound IAPP monomers (enriched at high zinc/IAPP stoichiometry) reduced IAPP self-association and aggregation as in the case of protonated His18 at low pH.[14] While DMD simulations offered an explanation for the concentration-dependent effect of zinc on IAPP aggregation as observed experimentally,[16,22–26] these results also suggest that zinc binding alone is insufficient for the endogenous inhibition of IAPP aggregation. C-peptide, on the other hand, was found to promote IAPP aggregation *in vitro*.[22] Hence, we *postulate* that the cooperative effect of zinc and C-peptide rather than individual molecules may be responsible for the endogenous inhibition of IAPP aggregation.

We first applied all-atom DMD simulations[27] to study the structure and dynamics of the various molecular systems comprised of zinc, C-peptide, and IAPP (details see Methods in ESI). To validate the aggregation promotion effect of C-peptide, we simulated the dimerization of IAPP with and without the presence of C-peptide. Indeed, C-peptide significantly accelerated the self-association of IAPP dimers (Fig. S1). However, C-peptide binding did not affect the secondary (Fig. S2A,B) and quaternary (Fig. S2C,D) structures of

the IAPP dimeric aggregates. This effect likely originated from electrostatic attractions as the net charge of IAPP is +2e (Lys1 and Arg11) while it is -5e for C-peptide (Glu1, Glu3, Asp4, Glu11, and Glu27).

It has been experimentally shown that all five acidic residues of C-peptide contribute to Zn^{2+} binding at a 1:1 stoichiometry.[28] Simulations of zinc, C-peptide, and IAPP at a 1:1:1 molecular ratio indicated that Zn^{2+} bound to C-peptide more rapidly than its binding with IAPP (Fig. S3A). The binding probability of Zn^{2+} with C-peptide approached 1, while the binding of Zn^{2+} with IAPP was only observed in ~40% simulations after 50 ns. The differential binding kinetics was due to the different driving forces, as C-peptide has five charged acidic residues all contributing to Zn^{2+} binding with a longer interaction range and larger binding cross-section, but the zinc-binding His18 of IAPP was neutral with a shorter interaction range and smaller binding cross section. Zn^{2+} bound preferentially to three N-terminal acidic residues of C-peptide due to their mutual proximity (Fig. S3B,C).

Since the coordination valence of Zn^{2+} is up to six[29] and Zn^{2+} in the heterodimer structures obtained above is solvent exposed (e.g., Fig. S4A), it is possible for Zn^{2+} to coordinate additional molecules. Given that Zn^{2+} bound C-peptide at 1:1 stoichiometry[28] while each zinc coordinated with at least three N-terminal acidic residues of C-peptide (Fig. S3B), we anticipated further coordination of zinc with additional IAPPs instead of C-peptides to form higher-order complexes. We also performed DMD simulations with one zinc, one C-peptide, and up to three IAPPs. With two IAPPs, the zinc ion became fully buried, preventing further coordination with additional IAPPs (e.g., Fig. S4B). Therefore, our simulations suggest that each zinc and C-peptide pair could coordinate up to two IAPPs, forming a heterodimer or a heterotrimer.

The heterotrimer had a significantly stronger energy gain upon complexation than the heterodimer, suggesting a higher thermodynamic stability of the heterotrimer (Fig. 1A). While N-terminal residues 6-15 and amyloidogenic region residues 21-30 adopted helical structures in both complexes, the heterotrimer was significantly more helical (Fig. 1B). The structural ensemble of the heterodimer was diverse with a high number of representative structures (e.g., the top tencentroid structures with clustering analysis in Fig. S5), suggesting a high structure flexibility. Contrarily, heterotrimer structures were well-defined (e.g., three lowest energy representative structures from clustering analysis in Fig. 1C), where each IAPP featured two helixes with the C-peptide separating the two peptides. Since the formation of inter-peptide hydrogen bonds especially between the amyloidogenic regions is important for amyloid fibrillization, the heterotrimer with stable helices in the amyloidogenic region is likely aggregation-incompetent.

We evaluated the nucleation propensity of both hetero-complexes *in silico* by testing whether the IAPPs in the complex can form inter-peptide hydrogen bonds with an additional IAPP. For the heterodimer, the binding between its IAPP and the incoming one was similar to that of two IAPP alone (Fig. S6). In contrast, IAPPs in the heterotrimer formed a much lower numbers of atomic contacts and inter-peptide hydrogen bonds with the incoming IAPP compared to both the heterodimer and the control simulations of IAPP dimerization. Together, the simulation results suggest that the formation of zinc-coordinated hetero-

complexes between IAPP and C-peptide, especially the stable the heterotrimer instead of the intermediate heterodimer, stabilize IAPP in a helical and aggregation-incompetent state.

Next, we applied ThT fluorescence assay, TEM imaging, and CD spectroscopy to test the effects of zinc and/or C-peptides on IAPP aggregations (ESI). Using a ThT fluorescence kinetic assay, we observed that in the presence of zinc (Zn), C-peptide, or both C-peptide and Zn (kept at 1:1 stoichiometry as previously reported[28]), IAPP fibrillization was increased or comparable with the control of IAPP alone after 14 h incubation, except for the molar ratios of 2.7:1:1 of IAPP/C-peptide/Zn where IAPP fibrillization was markedly decreased and its lag phase increased compared to the IAPP control (Fig. 2A, Fig. S7). Specifically, the ThT fluorescence intensity, which is proportional to the amount of beta-rich aggregates, increased at IAPP/C-peptide/Zn molar ratios of 0.3:1:1 and 0.7:1:1. At the molar ratios of 1.3:1:1 and 5.3:1:1, the fluorescence intensities for IAPP with C-peptide or both C-peptide and Zn were comparable to that for IAPP alone.

High-resolution transmission electron microscopy (TEM) imaging provided direct visualization of IAPP fibrillization and morphology such as fibril contour length, stiffness (evaluated by the persistence length λ[30,31]) and branching (Fig. 1B-F, Fig. S8). Consistently with the ThT assay for 14 h of incubation, TEM imaging revealed the formation of fibrils and aggregates at IAPP/C-peptide/Zn^{2+} molar ratios of 0.3:1:1, 0.7:1:1, 1.3:1:1, and 5.3:1:1, more prevalently than the IAPP control (Fig. S8). In contrast, we did not observe conventional fibrillar structures but the presence of small aggregates of 8.4 ± 2.7 nm in size at IAPP/C-peptide/Zn^{2+} molar ratios of 2.7:1:1 (10× magnification in Fig. 2B). Statistical analysis indicated that these aggregates were much softer (λ ~ 187 nm, Fig. 2C) than those of the IAPP control (λ ~ 2,885 nm), confirming their amorphous and non-fibrillar characteristics. IAPP fibrillization was persistent for IAPP/C-peptide of all tested molar ratios of 0.3:1 to 5.3:1 (Fig. 2B, Fig. S8), while fibril softening occurred also for all conditions (Fig. 2C). In addition, 24 h incubation of IAPP with Zn^{2+} either enhanced or inhibited IAPP fibrillization according to TEM imaging (Fig. 2B, Fig. S2M-Q), although 14 h incubation with Zn^{2+} caused modest IAPP fibrillization inhibition in the ThT assay (Fig. 2A). Here, the observed concentration-dependence for zinc on IAPP aggregation is consistent with our previous studies.[16] The experimentally observed 2.7:1 ratio with maximum aggregation inhibition is close to the predicted 2:1 molecular ratio between IAPP and C-peptide in the aggregation-incompetent heterotrimer (Figs. 1, 2).

Circular dichroism (CD) spectroscopy was utilized to assess the effects of zinc/C-peptide on the secondary structures of IAPP at different molar ratios (Fig. 3). The IAPP control showed a significant increase of β-sheet content from 31.8% to 77.4% coupled with a drastic decrease in random coil, indicating IAPP aggregation after 24 h incubation. 24 h incubation of IAPP/C-peptide/Zn^{2+} of 0.7:1:1, 1.3:1:1, 2.0:1:1 and 2.7:1:1 yielded significant reductions in the beta-sheet content and overall increases in turns and random coils. Specifically, IAPP/C-peptide/Zn at the molar ratio of 2.7:1:1 exhibited a marked decrease from 77.4% to 34.3% in beta-sheets along with an increase of alpha-helix from 18.5% to 25.3% and turns from 4.1% to 40.3%, displaying a non-fibrillar characteristics. Such contrasting conformational changes of IAPP at different IAPP/C-peptide/Zn molar ratios are consistent with the ThT and TEM results. Most importantly, the increase of helical content

at the 2.7:1:1 molecular ratio agrees with the predicted formation of stable α-helix in the IAPP amyloidogenic region upon zinc-coordinated C-peptide complexation (Fig. 1). At lower IAPP to Zn/C-peptide molecular ratios, the unstructured C-peptides in the solution resulted into reduced overall helical content and increased coil content (Fig. 3B). Therefore, although our atomistic DMD simulations only modelled simplified molecular systems due to computational limitations, our complementary biophysical experiments offered compelling evidence on the predicted IAPP stabilization via zinc-coordinated complexation with C-peptide.

We also performed a cell viability assay to assess the differential cytotoxicity of the various molecular species to insulin-secreting NIT-1 mouse pancreatic β-cell line. After 24 h incubation, the cells were exposed to DNA binding dyes Hoechst 33342 and propidium iodide. Hoechst 33342 freely diffuses into cells with preserved membranes, staining DNA blue. Propidium iodide is permeable to compromised cell membranes, staining DNA of dead cells red. Thus, viable cells were identified by their intact nuclei with blue fluorescence, whereas cell death was quantified by blue-red fluorescence or by fragmented blue nuclei on immunofluorescence and light microscopy. We found that the controls of C-peptide and Zn^{2+} induced little toxicity (<0.7%) in NIT-1 cells after 24 h of treatment, while the controls of IAPP and IAPP/Zn^{2+} (2.7:1) caused significant cell death at 22.2±6.5% and 30.3±8.1%, respectively (Fig. 4). The sample of IAPP/C-peptide (2.7:1) induced minor toxicity (~1.8%). In contrast, IAPP/C-peptide/Zn at 2.7:1:1 molar ratios elicited minimal cytotoxicity of ~1.1±0.2%, indicating remarkable mitigation of IAPP toxicity through zinc-coordinated IAPP/C-peptide complexation. These *in vitro* results vindicate *in silico* prediction as well as ThT, TEM, and CD observations.

Conclusions

In summary, the zinc-coordinated heterotrimer with one C-peptide and two IAPPs was both thermodynamically and structurally stable, where the amyloidogenic region of IAPP assumed stable helices and the complex was aggregation-incompetent. IAPP/C-peptide/Zn mixture at 2.7:1:1 molecular ratios significantly reduced the cytotoxicity of IAPP. In light of the coexistence of high concentrations of zinc, C-peptide, and IAPP inside β-cell granules, this study suggests that zinc-coordinated complexation between IAPP and C-peptide may play an important role in the native inhibition of IAPP aggregation, in addition to the reported low pH effect.[15] With future *in vivo* verifications and structural characterizations of the molecular complex, therapeutic approaches mimicking or promoting such zinc-coordinated molecular complexes may prove potent for the mitigation of aggregation-induced beta-cell death in T2D.

Supplementary Material

Refer to Web version on PubMed Central for supplementary material.

Acknowledgments

The work is partially supported by ARC Project No. CE140100036 (Davis), NSF CAREER CBET-1553945 (Ding), NIH R35GM119691 (Ding), NHMRC Project Grant APP1071350 (Gurzov), and an internal grant from Monash

Institute of Pharmaceutical Sciences (Ke). Gurzov is supported by a Juvenile Diabetes Research Foundation (JDRF) fellowship. The content is solely the responsibility of the authors and does not necessarily represent the official views of NIH and NSF.

Notes and References

1. Eisenberg D, Jucker M. Cell. 2012; 148:1188–1203. [PubMed: 22424229]
2. Knowles TPJ, Vendruscolo M, Dobson CM. Nat Rev Mol Cell Biol. 2014; 15:384–396. [PubMed: 24854788]
3. Ke PC, Sani MA, Ding F, Kakinen A, Javed I, Separovic F, Davis TP, Mezzenga R. Chem Soc Rev. 2017 in press.
4. Schmitz O, Brock B, Rungby J. Diabetes. 2004; 53:S233–S238. [PubMed: 15561917]
5. Zraika S, Hull RL, Verchere CB, Clark A, Potter KJ, Fraser PE, Raleigh DP, Kahn SE. Diabetologia. 2010; 53:1046–1056. [PubMed: 20182863]
6. Ritzel RA, Meier JJ, Lin CY, Veldhuis JD, Butler PC. Diabetes. 2007; 56:65–71. [PubMed: 17192466]
7. Hutton JC. Diabetologia. 1989; 32:271–281. [PubMed: 2526768]
8. Hutton JC. Biochem J. 1982; 204:171–178. [PubMed: 6126183]
9. DeToma AS, Salamekh S, Ramamoorthy A, Lim MH. Chem Soc Rev. 2012; 41:608–621. [PubMed: 21818468]
10. Chimienti F, Favier A, Seve M. Biometals. 2005; 18:313–317. [PubMed: 16158222]
11. Lemaire K, Ravier MA, Schraenen A, Creemers JWM, Van de Plas R, Granvik M, Van Lommel L, Waelkens E, Chimienti F, Rutter GA, Gilon P, in't Veld PA, Schuit FC. Proc Natl Acad Sci U S A. 2009; 106:14872–14877. [PubMed: 19706465]
12. Wahren J, Ekberg K, Johansson J, Henriksson M, Pramanik A, Johansson BL, Rigler R, Jörnvall H. Am J Physiol Endocrinol Metab. 2000; 278:E759–768. [PubMed: 10780930]
13. Larson JL, Miranker AD. J Mol Biol. 2004; 335:221–231. [PubMed: 14659752]
14. Abedini A, Raleigh DP. Biochemistry. 2005; 44:16284–16291. [PubMed: 16331989]
15. Khemtémourian L, Doménech E, Doux JPF, Koorengevel MC, Killian JA. J Am Chem Soc. 2011; 133:15598–15604. [PubMed: 21870807]
16. Nedumpully-Govindan P, Yang Y, Andorfer R, Cao W, Ding F. Biochemistry. 2015; 54:7335–7344. [PubMed: 26603575]
17. Nedumpully-Govindan P, Ding F. Sci Rep. 2015; 5:8240. [PubMed: 25649462]
18. Gilead S, Wolfenson H, Gazit E. Angew Chem Int Ed Engl. 2006; 45:6476–6480. [PubMed: 16960910]
19. Susa AC, Wu C, Bernstein SL, Dupuis NF, Wang H, Raleigh DP, Shea JE, Bowers MT. J Am Chem Soc. 2014; 136:12912–12919. [PubMed: 25144879]
20. Brender JR, Lee EL, Hartman K, Wong PT, Ramamoorthy A, Steel DG, Gafni A. Biophys J. 2011; 100:685–692. [PubMed: 21281583]
21. Jha S, Snell JM, Sheftic SR, Patil SM, Daniels SB, Kolling FW, Alexandrescu AT. Biochemistry. 2014; 53:300–310. [PubMed: 24377660]
22. Westermark P, Li ZC, Westermark GT, Leckström A, Steiner DF. FEBS Lett. 1996; 379:203–206. [PubMed: 8603689]
23. Brender JR, Hartman K, Nanga RPR, Popovych N, de la Salud Bea R, Vivekanandan S, Marsh ENG, Ramamoorthy A. J Am Chem Soc. 2010; 132:8973–8983. [PubMed: 20536124]
24. Brender JR, Krishnamoorthy J, Messina GML, Deb A, Vivekanandan S, Rosa CL, Penner-Hahn JE, Ramamoorthy A. Chem Commun. 2013; 49:3339–3341.
25. Salamekh S, Brender JR, Hyung SJ, Nanga RPR, Vivekanandan S, Ruotolo BT, Ramamoorthy A. J Mol Biol. 2011; 410:294–306. [PubMed: 21616080]
26. Brender JR, Salamekh S, Ramamoorthy A. Acc Chem Res. 2012; 45:454–462. [PubMed: 21942864]
27. Ding F, Tsao D, Nie H, Dokholyan NV. Structure. 2008; 16:1010–1018. [PubMed: 18611374]

28. Keltner Z, Meyer JA, Johnson EM, Palumbo AM, Spence DM, Reid GE. Analyst. 2010; 135:278–288. [PubMed: 20098759]
29. Laitaoja M, Valjakka J, Jänis J. Inorg Chem. 2013; 52:10983–10991. [PubMed: 24059258]
30. Adamcik J, Jung JM, Flakowski J, De Los Rios P, Dietler G, Mezzenga R. Nat Nanotechnol. 2010; 5:423–428. [PubMed: 20383125]
31. Usov I, Mezzenga R. Macromolecules. 2015; 48:1269–1280.

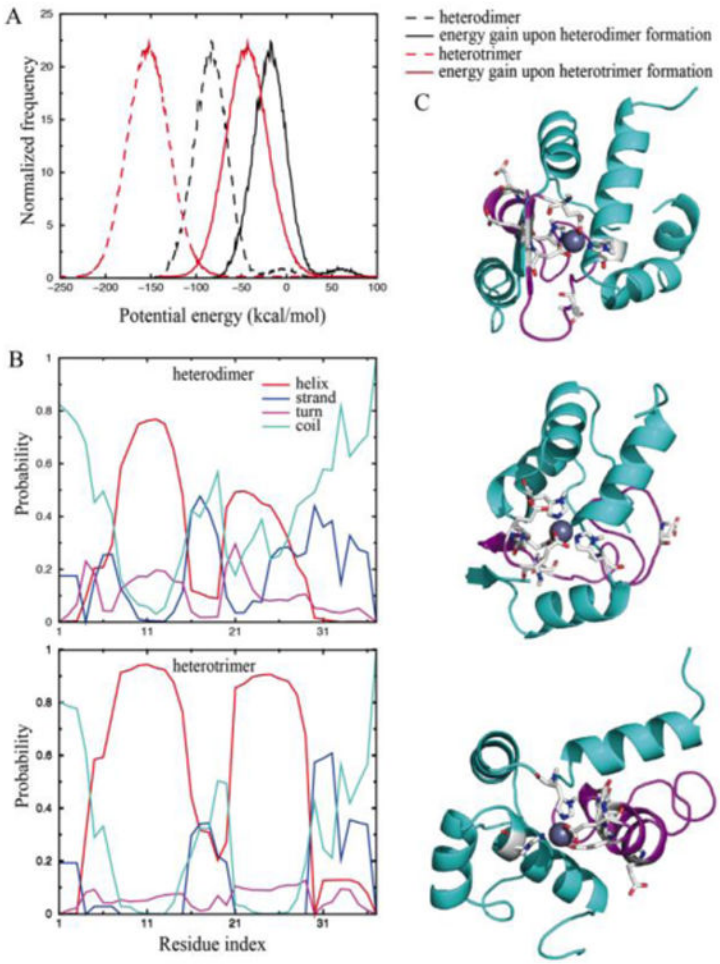

Figure 1.

DMD simulations of the heterotrimer. (A) The energy gains upon complexation. (B) Secondary structure contents of IAPP in the heterodimer (upper) and heterotrimer (lower). (C) Representative structures of a heterotrimer. IAPP is coloured in cyan while C-peptide in magenta. Zinc-binding residues are highlighted as sticks.

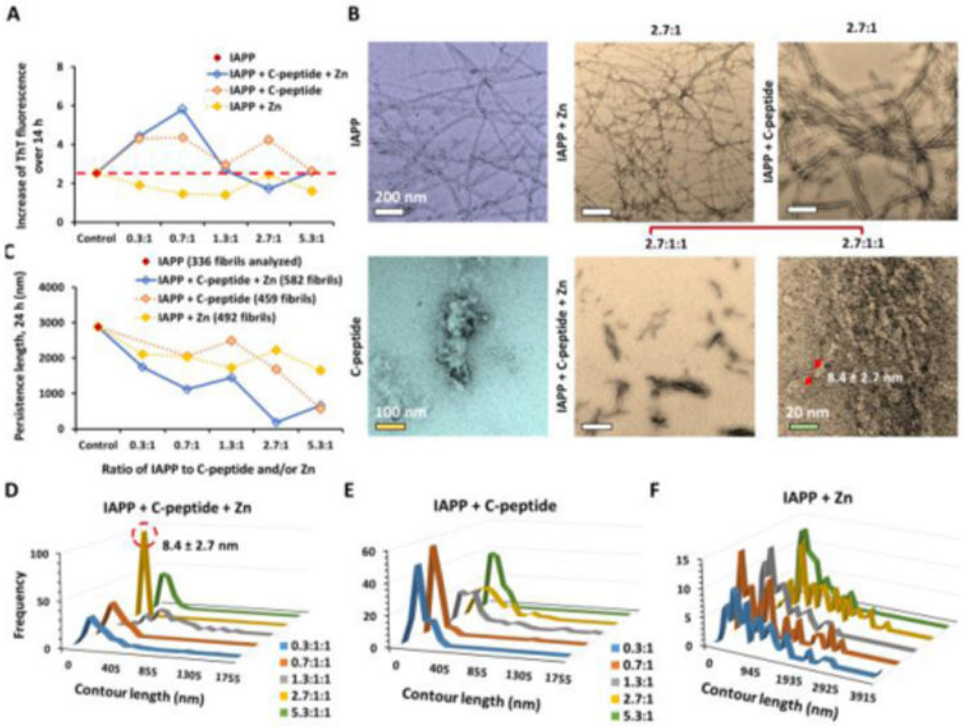

Figure 2.

Experimental studies of zinc-coordinated IAPP-C-peptide complexation. (A) ThT fluorescence assay for 14 h of sample incubation. The time dependent data are shown in Fig. S1. (B) TEM imaging of IAPP aggregation after 24 h incubation with zinc (Zn) and/or C-peptide. Only the samples with molecular ratio of 2.7:1 are shown while the rest is in Fig. S2. (C-F) Statistical analysis of the persistence length and contour length of IAPP fibrils. The concentration of IAPP was kept 16.9 μM in all samples.

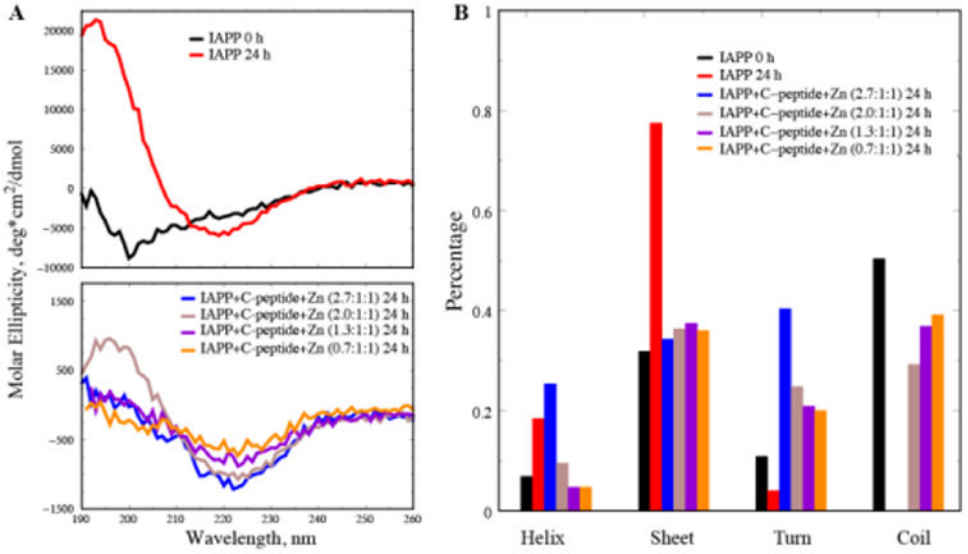

Figure 3.

CD measurement of the secondary structures of IAPP control and IAPP/C-peptide/Zn^{2+} mixtures. (A) IAPP control of 25 μM at 0 h and 24 h incubation (upper), and IAPP/C-peptide/Zn^{2+} at different molar ratios after 24 h incubation (lower). (B) Secondary structural contents for the various molecular systems.

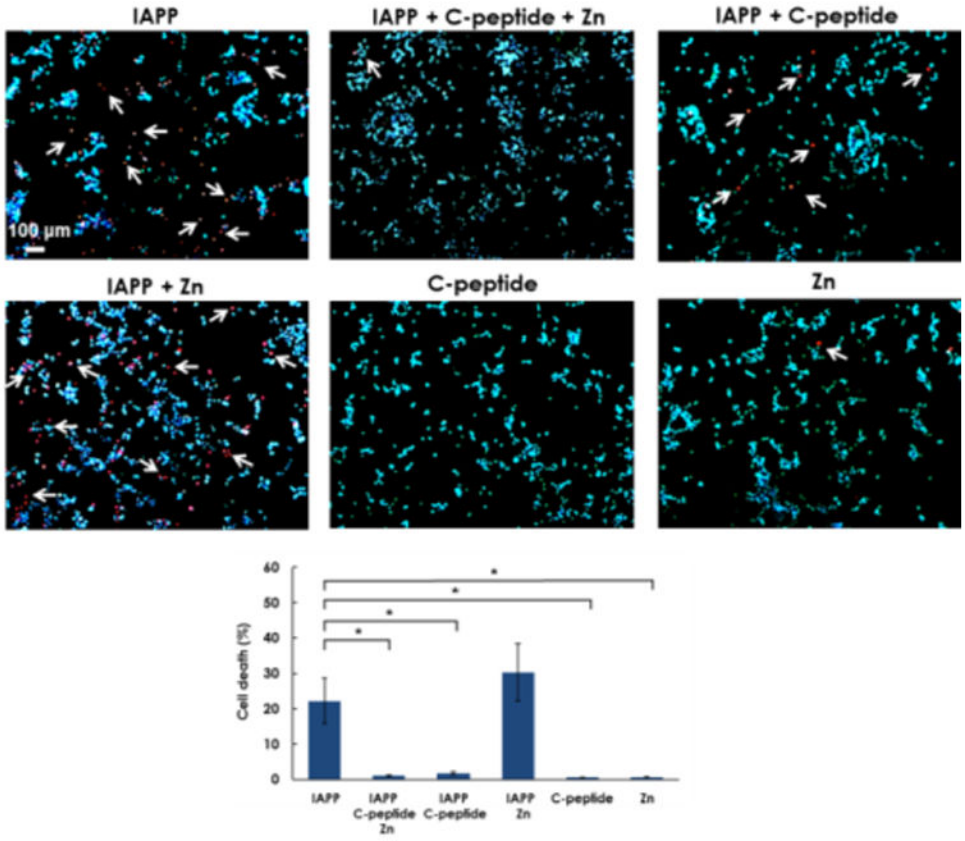

Figure 4.

C-peptideprotects β-cells from IAPP-induced cell death. NIT-1 cells were untreated (control) or incubated with IAPP, C-peptide, Zn or combination as indicated for 24 h. Cell death was evaluated by Hoechst-33342 (blue)/propidium iodide (red). White arrows indicate propidium iodide positive cells. Data shown are means ± SEM of 4 independent experiments. $*P < 0.05$.